Fast and Accurate Calculation of Mutual Inductance in the Presence of Conductive and Magnetic Media

Dyuti Sengupta and Andreas Weisshaar
School of Electrical Engineering and Computer Science
Oregon State University
Corvallis, Oregon 97331, USA
Email: andreas@oregonstate.edu

***Abstract*—This paper presents a complex image approach for fast and accurate calculation of the mutual inductance between two coils in the presence of conductive and magnetic layered media. The complex images are obtained by application of Prony's method to the spectral domain form of the vector magnetic potential. The accuracy of the method is demonstrated by comparison of the mutual inductance between two coaxial coils separated by a conductive medium with the electromagnetic fullwave simulator HFSS as well as with published measurement data. The technique is general, versatile, and fast and has wide applicability, including in wireless power transfer and shielding.**

***Index Terms*—mutual inductance, complex image method, Prony's method, complex inductance, conductive medium**

I. Introduction

With the recent developments and increasing interest in magnetic near-field-coupling-based systems for wireless power transfer and magnetic shielding in diverse application environments, accurate modeling of magnetic flux transmission through various types of layered media (metal sheets, conductive and magnetic materials and even metamaterials) is becoming essential for designing highly efficient systems. Precise calculation of the coupling inductance in such environments generally requires the application of complex mathematical functions or extensive electromagnetic (EM) simulations, making these methods time and memory intensive for highly evolved systems.

To address the lack of a general and efficient method for mutual inductance calculations in the presence of conductive and magnetic media, we present in this paper a highly efficient and versatile method to analyze the magnetic flux transmission and determine the mutual inductance of a two-coil system by extending the concept of complex image theory and applying Prony's method of approximation. Our method is applicable to environments with general conductive and magnetic media and can model both magnetic flux enhancement and shielding. Comparative analyses between the results obtained using our innovative method, full wave 3D EM simulations and measurements demonstrate the high level of efficiency of our approach.

II. Problem Formulation

Figure 1 shows the general configuration of two coils separated by a layer of conductive and/or magnetic medium.

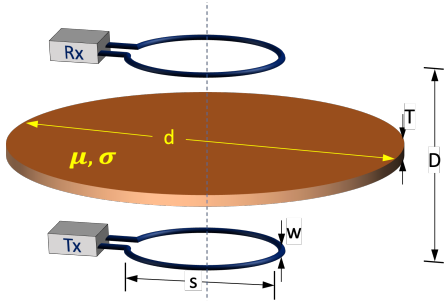

Fig. 1. General problem setup of inductive coupling between two coils through a conductive and magnetic medium.

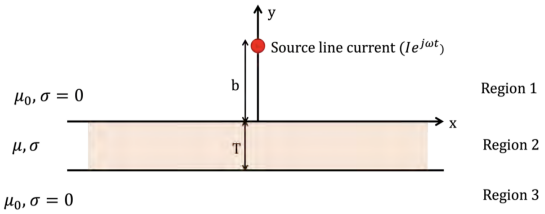

Fig. 2. Line current above a general conductive and magnetic slab.

The mutual inductance can be calculated in terms of vector magnetic potential $\vec{A}$ as

$$M = L_{21} = \frac{1}{I_1} \oint_{C_1} \vec{A}_1 \cdot \vec{dl} \tag{1}$$

where I_1 is the current in coil Tx (coil 1) and C_2 is the contour path along coil Rx (coil 2). Analytical solutions for the mutual inductance between two coils are available for various configurations in free-space [1]–[5]; however, in the presence of conductive or magnetic media, the solution approaches are cumbersome and limited.

In order to develop a fast calculation approach based on the complex image theory, consider a filamental line current in the z-direction above a general conductive and magnetic slab of thickness T, as illustrated in Fig. 2. The vector magnetic potential in the three different regions ($i = 1, 2, 3$) satisfies

$$\nabla^2 A_{z,i}(x,y) - j\omega\mu_i\sigma_i A_{z,i}(x,y) + \mu_0 I\delta(x)\delta(y-b) = 0 \quad (i = 1,2,3). \tag{2}$$

979-8-3503-1798-5/23/$31.00 ©2023 IEEE

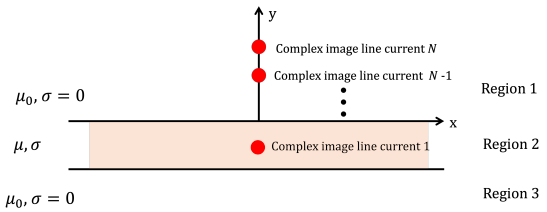

(a)

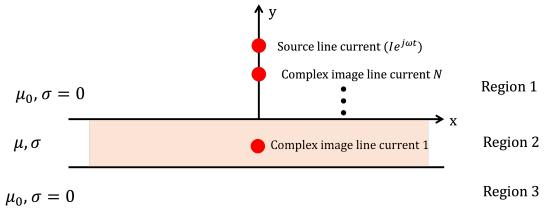

(b)

Fig. 3. Complex image approximation for problem setup shown in Fig. 2 for: (a) $G(k)$, (b) $H(k)$.

The solution for the vector magnetic potential in region 3 is found as [6], [7]

$$A_{z,3}(x,y) = \frac{\mu_0 I}{2\pi}\int_0^\infty \left[G(k)\frac{e^{k(y-b)}}{k}\right]\cos(kx)dk \quad (3)$$

where $G(k)$ is a spectral function given by

$$G(k) = 4kq\frac{\mu_r e^{kT}}{(q+\mu_r k)^2 e^{qT} - (q-\mu_r k)^2 e^{-qT}} \quad (4)$$

with $q = \sqrt{k^2+\gamma^2}$ and $\gamma = \sqrt{j\omega\mu\sigma}$. Spectral function $G(k)$ represents the effect of the source current and the conductive and magnetic slab on the magnetic fields. Note that in the case of free space, $G(k) = 1$. Alternatively, we can define spectral function $H(k) = 1 - G(k)$ to separate out the effect of the slab medium from the total solution. This form of solution is preferable for media with low losses where the source term is dominant.

III. Complex Image Approximation

In [8] and [9], the spectral function for the vector magnetic potential solution in the source region was approximated by a single complex image which was obtained by Taylor series expansion. Here, we approximate the spectral function $G(k)$ (or $H(k)$) of the quasi-magnetostatic formulation as the sum of N complex exponential solutions given as

$$G(k = mT_s) \approx \sum_{n=1}^{N} A_n e^{j\theta_n} e^{(\alpha_n + j2\pi f_n)mT_s} \quad (5)$$

by application of Prony's method [10], [11]. In (5) A_n and θ_n are the initial amplitude and phase, respectively, while α_n is the damping factor, f_n is the frequency, T_s is the sampling period, and $m = 0, 1, 2, \ldots$. The complex exponentials (when divided by k in (3)) represent image source currents in the real domain with complex amplitude and at a complex location.

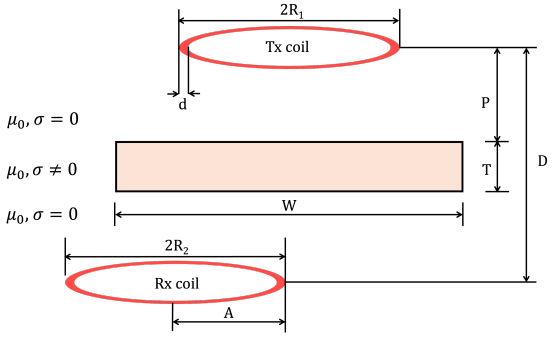

Fig. 4. Illustration of two coils offset by distance A with a layer of general conductive medium of thickness T.

For a two-coil system with conductive slab, as shown in Fig. 4, the problem can now be replaced with a set of N image coils ($n = 1, \cdots, N$) in free space, each with complex source current $A_n e^{j\theta_n} I$ and placed at a complex distance $D_c(n)$ from the Rx coil given by

$$D_c(n) = D - (\alpha_n + j2\pi f_n) \quad (6)$$

where D is the distance between the Tx coil (coil 1) and Rx coil (coil 2). The resulting total complex coupling inductance L_{21}^* between the two coils can then readily be obtained as the sum of all complex mutual inductances M_n^* between image Tx coil n ($n = 1, \cdots, N$) and the Rx coil, as given by

$$L_{21}^* = \sum_{n=1}^{N} \left(A_n e^{j\theta_n} M_n^*\right). \quad (7)$$

The corresponding mutual impedance Z_{21} between the Tx coil (coil 1) and Rx coil (coil 2) in the presence of the conductive and magnetic medium is obtained from L_{21}^* as

$$Z_{21} = j\omega L_{21}^* = R_{21} + j\omega L_{21} = -\omega\,\mathrm{Im}\{L_{21}^*\} + j\omega\,\mathrm{Re}\{L_{21}^*\} \quad (8)$$

For the case of coaxial Tx and Rx coils in a general layered medium, as illustrated in Fig. 4 with zero offset ($A = 0$), closed-form formulas for the mutual inductance between coaxial coils in free space [1] are evaluated with complex distance $D_c(n)$ given in (6) for each image coil. Thus, the total complex inductance L_{21}^* is given in closed form as

$$\begin{aligned} L_{21}^* = \sum_{n=1}^{N} \{ & A_n e^{j\theta_n} \mu_0 \sqrt{R_1 R_2} \\ & \times \left[\left(\frac{2}{\nu(n)} - \nu(n)\right) K(\nu(n)) - \frac{2}{\nu(n)} E(\nu(n))\right]\} \end{aligned} \quad (9)$$

where

$$\nu(n) = \sqrt{\frac{4R_1R_2}{(D_c(n))^2 + (R_1+R_2)^2}} \quad (10)$$

and $E(\nu)$ and $K(\nu)$ are the complete elliptical integrals of the first and second kind, respectively ([1]). A similar formulation is obtained for the case of misaligned coils using the results for the free-space case established in [2]–[5].

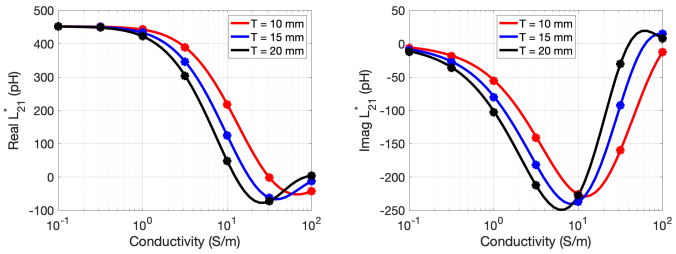

(a) (b)

Fig. 5. Complex mutual inductance L_{21}^{*} for aligned coaxial Tx and Rx coils in the presence of a conductive medium layer (see Fig. 4 with $A = 0$, $D = 37$mm, $R_1 = R_2 = 11$mm, $d = 0.1$mm, $P = 5$mm, $W = 250$mm, $f = 159$MHz. Model results given by solid lines, HFSS results by symbols).

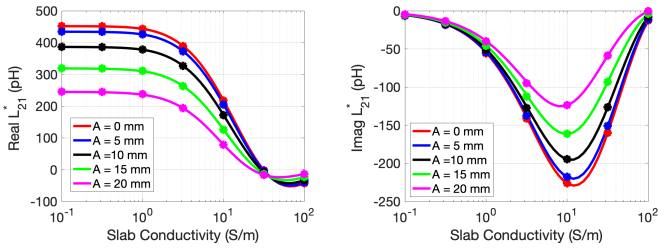

(a) (b)

Fig. 6. Complex mutual inductance L_{21}^{*} for misaligned Tx and Rx coils in the presence of a conductive medium layer for different amounts of offset A (see Fig. 4 with $D = 37$mm, $R_1 = R_2 = 11$mm, $d = 0.1$mm, $T = 10$mm, $P = 5$mm, $W = 250$mm, $f = 159$MHz. Model results given by solid lines, HFSS results by symbols).

IV. Applications

We have applied the complex image approach to efficiently determine the complex mutual inductance between two coils in the presence of a layer of conductive medium as shown in Fig. 4. The model results are compared with fullwave simulation results obtained with HFSS [12]. Figure 5 shows the real and imaginary parts of the mutual inductance as a function of conductivity of the slab for different slab thicknesses. Similarly, Fig. 6 shows the complex mutual inductance as a function of slab conductivity for different lateral offsets between the coils. In all cases, the agreement of the model results with the fullwave HFSS simulation results is excellent. Figure 7 shows a comparison with measurement results taken from [13] for the setup in Fig. 1. Included in the figure are the results of the generalized Dodd & Deeds formulation that includes retardation effects [14] and CST Microwave Studio [15] taken from [13]. Our model results are in good agreement with the measured results and our HFSS simulation results; the small differences can be attributed to the finite size of the conductive disk and the high dielectric constant of the medium.

V. Conclusion

We have presented a complex image approach based on Prony's method for the fast and accurate calculation of the mutual inductance between conductor coils in the presence of a conductive and magnetic layered medium. Our method can

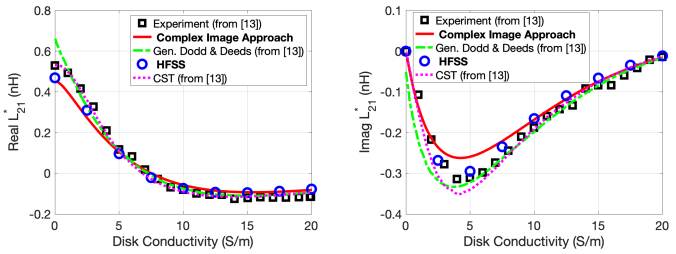

(a) (b)

Fig. 7. Complex mutual inductance for the configuration shown in Fig. 1 taken from [13] with $d = 37$mm, $s = 22$mm, $w = 1$mm, $T = 30$mm, $D = 90$mm, $f = 159$MHz.

be applied to general coil configurations and provides quick solutions to problems for which otherwise only complicated analytical methods or numerical methods are available. The approach can also be extended to general multi-layered media and problems involving metamaterials, as demonstrated in [16]. This complex image approach is widely applicable including in wireless power transfer and shielding problems.

References

[1] S. Ramo, J. R. Whinnery, and T. Van Duzer, *Fields and Waves in Communication Electronics,* 3rd ed. New York: Wiley, 1994.

[2] F. W. Grover, "The Calculation of the Mutual Inductance of Circular Filaments in Any Desired Positions," *Proc. IRE*, vol. 32, no. 10, pp. 620–629, Oct. 1944.

[3] F. W. Grover, *Inductance Calculations: Working Formulas and Tables*, Dover, New York, 1962.

[4] S. I. Babic, F. Sirois, and C. Akyel, "Validity Check of Mutual Inductance Formulas for Circular Filaments with Lateral and Angular Misalignments," *Prog. Electromagn. Res. M*, Vol. 8, 15–26, 2009.

[5] C. Akyel, S. I. Babic, and M.-M. Mahmoudi, "Mutual Inductance Calculation for Non-Coaxial Circular Air Coils with Parallel Axes," Progress In Electromagnetics Research, Vol. 91, 287-301, 2009.

[6] J. A. Tegopoulos and E. E. Kriezis, *Eddy Currents in Linear Conducting Media.* Amsterdam: Elsevier, 1985.

[7] E. Grotelüschen, et al., "Full-wave analysis and analytical formulas for the line parameters of transmission lines on semiconductor substrates," *Integration, the VLSI journal,* vol. 16, pp. 33-58, 1993.

[8] A. Weisshaar, H. Lan, and A. Luoh, "Accurate Closed-Form Expressions for the Frequency-Dependent Line Parameters of Coupled On-Chip Interconnects on Lossy Silicon Substrate," *IEEE Trans. Adv. Packaging*, vol. 25, No. 2, pp. 288–296, May 2002.

[9] A. Weisshaar and A. Luoh, "Closed-form expressions for the series impedance parameters of on-chip interconnects on multilayer silicon substrates," *IEEE Trans. Adv. Packaging*, vol. 27, no. 1, pp. 126–134, Feb. 2004.

[10] J. J. Yang, et al., "Discrete complex images of a three-dimensional dipole above and within a lossy ground," IEE Proc-H, Vol. 138, No. 4, pp. 319–326, Aug. 1991.

[11] F. Rodríguez, et al., "Coding Prony's method in MATLAB and applying it to biomedical signal filtering," *BMC Bioinformatics* 19, 451 (2018).

[12] HFSS (2022R2). ANSYS. [Online]. https://www.ansys.com/products/electronics/ansys-hfss.

[13] A. Vallecchi, S. Chu, L. Solymar, C. J. Stevens and E. Shamonina, "Coupling between coils in the presence of conducting medium," *IET Microw. Antennas Propag.*, vol. 13, no. 1, pp. 55–62, Sep. 2018.

[14] C. V. Dodd, and W. E. Deeds, "Analytical solutions to eddy current coil problems," *J. Appl. Phys.*, pp. 2829–2838, 1968.

[15] CST Microwave Studio, User Manual, 2017.

[16] D. Sengupta, "Enhanced Modeling and Design of Magnetic Coupling Systems for Wireless Power Transfer and Shielding," Ph.D. dissertation, Oregon State University, March 2023.